Scanning Electron Microscope Study of the Root-knot Nematode (Meloidogyne incognita) on Tomato Root[1]

W. P. Wergin and D. Orion[2]

Abstract: This study examines the types of structural information that can be gained by utilizing the scanning electron microscope (SEM) and a cryofracture technique to examine the host-parasite interaction. Roots of tomato, *Lycopersicon esculentum* cv. Marglobe, were cultured aseptically and inoculated with the root-knot nematode, *Meloidogyne incognita*. Twenty-four hours to four weeks after inoculation, developing galls were removed from the cultures and processed for SEM observation. The cryofracture technique was used to reveal internal structural features within the developing galls. The results illustrate structural details concerning penetration of the roots, differentiation of syncytia, and development of the nematodes beginning with the second-stage larvae and ending with adult egg-laying females. *Key words: Meloidogyne incognita, Lycopersicon esculentum*, root-knot nematode, scanning electron microscopy, cryofracture.

Within the past 10 yr, the scanning electron microscope (SEM) has become an increasingly important research tool for nematologists. This instrument, which has a 20-fold increase in resolution over that of the light microscope and an exceptional depth of field, is currently being used to describe the surface features of nematodes in numerous laboratories. These studies are having a significant impact on nematode taxonomy.

Exceptions to the taxonomic applications of the SEM are the investigations by Jones et al. (6,7,9) and Orion et al. (11). Jones and coworkers carefully split roots infected with nematodes and then digested the plant cytoplasm to reveal the cell wall structure of the syncytia. These studies, which compared the wall structures in syncytia that are produced by several species of nematodes, have increased our understanding of the cell wall perforations that may result from enzymatic activity, as well as the cell wall ingrowths that appear to function in solute transport. In the study by Orion et al. (11), scanning microscopy was utilized to compare the influence of growth media on the gross morphology of syncytia. However, the SEM has not been used to examine other aspects of the host-parasite interaction involving nematodes and crop plants. For this reason a study was undertaken with this technique to illustrate the types of structural information that can be observed during penetration, feeding, and development of the nematode in plant tissue. A cryofracture technique, previously described for examining internal tissues of nematodes (5,14) and infected roots (14), was used to minimize the structural damage that could occur if these tissues were simply cut with razor blades or scalpels.

MATERIALS AND METHODS

Seeds of tomato, *Lycopersicon esculen-*

Received for publication 18 November 1980.

[1]This study is supported in part by the U.S. Department of Agriculture Competitive Grants Program, Agreement No. 5901-0410-9-0255-0 and the United States-Israel Agricultural Research and Development Fund-BARD, Grant No. I-96-80. No endorsements are implied herein.

[2]Nematology Laboratory, Plant Protection Institute, USDA SEA AR, Beltsville, MD 20705; and Division of Nematology, Institute of Plant Protection, Agricultural Research Organization, Volcani Center, Bet-Dagan, Israel, respectively. The authors thank Mr. B. F. Ingber for his technical assistance, and Dr. L. R. Krusberg for arranging a cooperative research agreement with the University of Maryland.

Figs. 1–2. Second stage larvae (*Meloidogyne incognita*) penetrating roots of tomato (*Lycopersicon esculentum*). In general, the larvae appear to penetrate intercellularly causing minor damage to adjacent cells (Fig. 1). However, occasional examples indicate that the epidermal cells around the penetration site are disrupted. This may result from probing before penetration, multiple infections at a single site, or from physical pressure exerted from movement along the body of the nematode as it enters the root. Fig. 1, ×550; Fig. 2, ×600.

Fig. 3. Portion of a root 48 hr after the culture was inoculated with an egg mass. At this time, radial swelling, which is characteristic of the infection site, can be observed. In addition, root hair development appears to be stimulated on the surface of the developing gall. ×75.

Fig. 4. Cryofractured section of a root 1 wk after inoculation. By this time a well formed syncytium consisting of several cells has developed in the vascular cylinder. ×150.

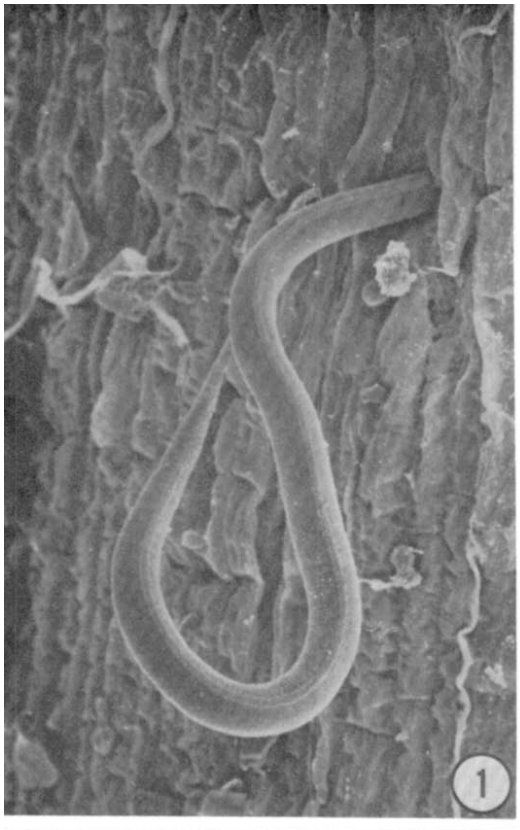
1

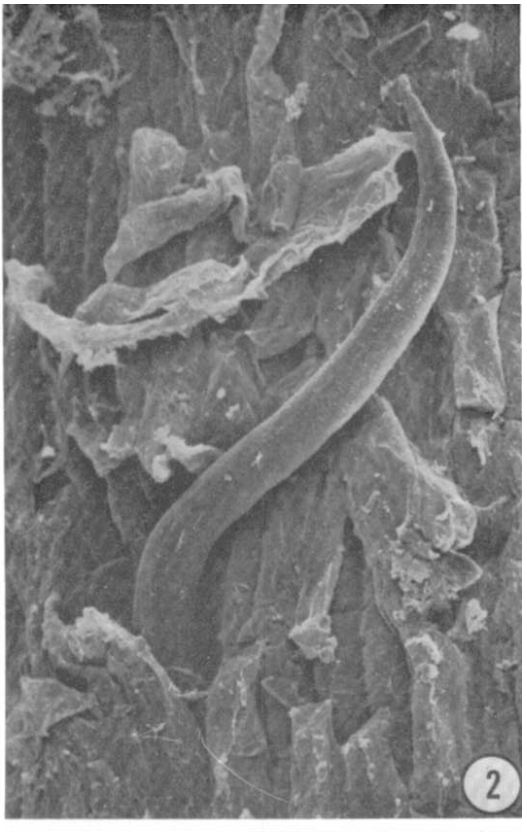
2

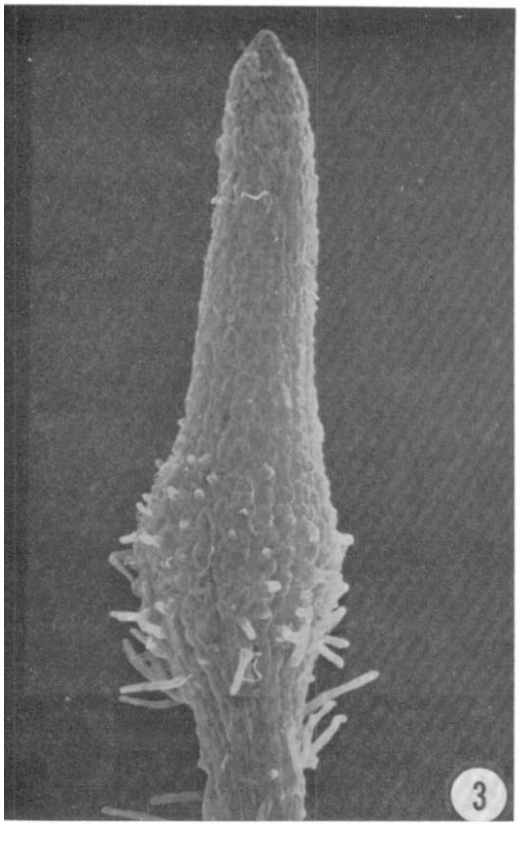
3

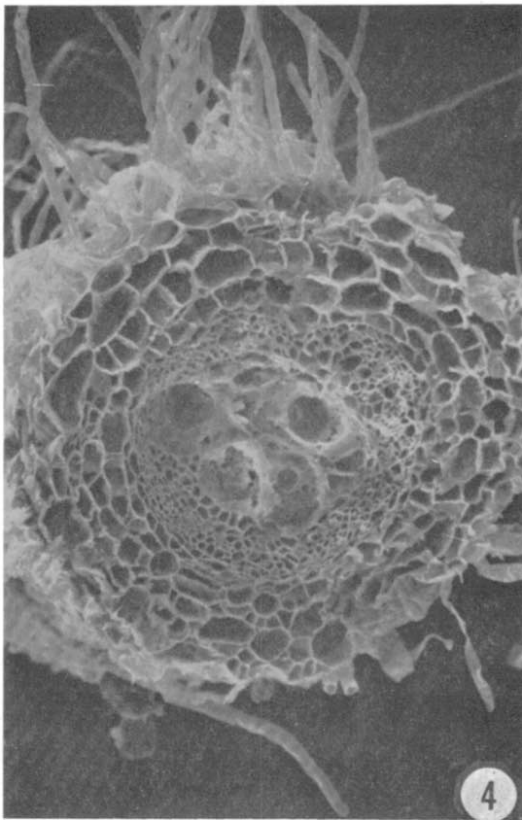
4

tum cv. Marglobe, were surface sterilized with 1% $NaClO_3$ solution for 15 min, rinsed three times with distilled water and placed in petri dishes containing 1% water agar. After the seeds germinated, 1 cm lengths of the primary root tip were excised and transferred to petri dishes containing a chemically defined medium formulated by Skoog, Tsui, and White (13). After lateral roots had emerged, they were inoculated by placing egg masses of *Meloidogyne incognita,* obtained from monoxenic cultures, 1–2 cm from the plant tissue. All cultures containing roots and/or nematodes were incubated in the dark at 25 C.

At 24 h, 48 h, 1, 2, 3, and 4 wk after inoculation, root samples were removed from the cultures and prepared for observation with the scanning electron microscope. To prepare the tissue, root segments containing galls were quickly removed from the cultures and placed in vials containing 3% glutaraldehyde in 0.05 M phosphate buffer, pH 6.8 at 22 C. Chemical fixation for 2–24 hr was followed by dehydration in a graded series of ethanol. The galled tissues were transferred from 100% ethanol to liquid nitrogen and fractured by exerting pressure with a scalpel while the roots were being observed with a stereoscopic light microscope. The fractured segments of the gall were then thawed in a fresh solution of 100% ethanol and critical point dried from liquid carbon dioxide. Next the gall segments were placed on stubs and coated with 20–30 nm of gold-palladium in a Technics Hummer V* sputtering device (Technics; 5510 Vine Street; Alexandria, VA 22310). The coated specimens were viewed in a Hitachi HHS-2R* scanning electron microscope operating at 10 or 15 kV (Hitachi Scientific Instruments, 460 East Middlefield Road, Mountain View, CA 94043).

RESULTS

24–48 hours: Within 24 h after inoculation, infective larvae can be observed penetrating the cortical region of the root. Examination of the root tissue around the penetration site reveals that in some instances the nematode enters between two adjacent epidermal cells causing little apparent damage to adjacent tissues (Fig. 1). In other examples, disruption and loss of the epidermis and underlying cortical cells may occur before penetration of the root by the nematode is successful (Fig. 2). Twenty-four to forty-eight hours after penetration, the infected roots exhibit radial swelling. The swelling, which normally occurs 1–4 mm back from the root tip in the region of maturation, is accompanied by a proliferation of root hairs on the surface of the forming gall (Fig. 3).

One week: One week after infection, cross sections through the swollen galls reveal well-formed syncytia in the vascular cylinders of the roots (Fig. 4). These syncytia consist of four to six giant cells that are 40–80 μm in diameter and have dense contents. Their larger sizes and characteristic contents easily distinguish them from the smaller highly vacuolated cells of the vascular cylinder.

The organelle content of the giant cells cannot be resolved; however, these cells do contain numerous small spherical bodies resembling vacuoles (Fig. 5). No obvious structural modification can be identified along the inner cell walls that separate the giant cells from the vascular tissue. How-

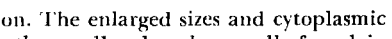

Fig. 5. Fractured section through a syncytium 1 wk after inoculation. The enlarged sizes and cytoplasmic contents of the cells in the syncytium are easily distinguished from the smaller, less dense cells found in normal vascular tissue. After 1 wk, xylem tissue (arrows) begins to differentiate adjacent to the syncytial tissue. ×500.

Fig. 6. Peripheral region of a syncytial cell (right) and the adjacent vascular tissue (left). The syncytial cell has a dense cytoplasm whose contents cannot be identified with the scanning electron microscope (SEM). The spherical areas within the cytoplasm may be small vacuoles (V) which are characteristic of the syncytial cells. The outer wall of the syncytium is contiguous with the walls of the adjacent vascular cells which develop into xylem tissue (X). ×2400.

Figs. 7–8. Cryofractured section of a root gall 2 wk after inoculation. No obvious changes occur in the size and number of cells found in the syncytium (Fig. 7). However, finger-like projections (arrows) 0.5 μm wide and 1–2 μm long develop along the inner wall of the syncytium, while xylem tissue (X) continues to form adjacent and appressed to the outer wall (Fig. 8). Fig. 7, ×125; Fig. 8, ×6000.

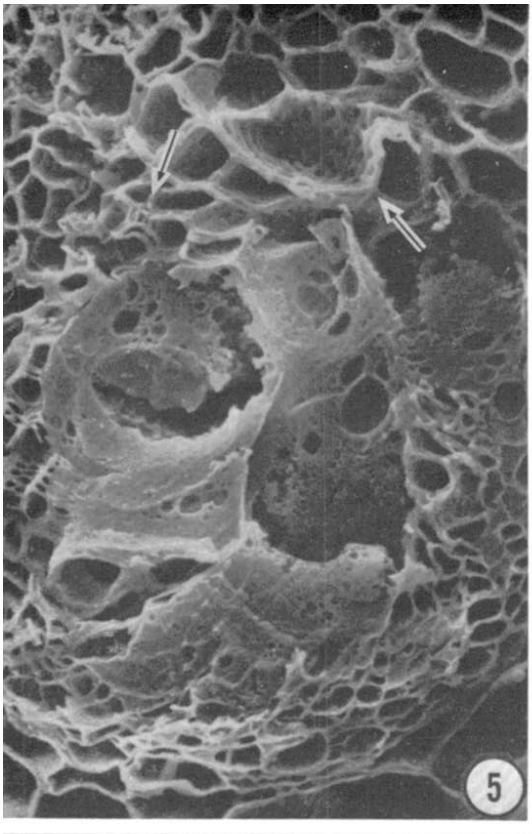
5

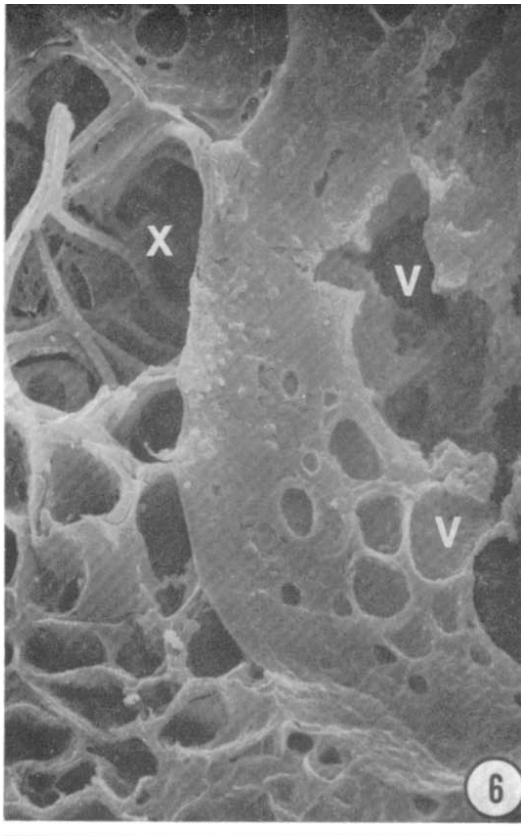
X
V
V
6

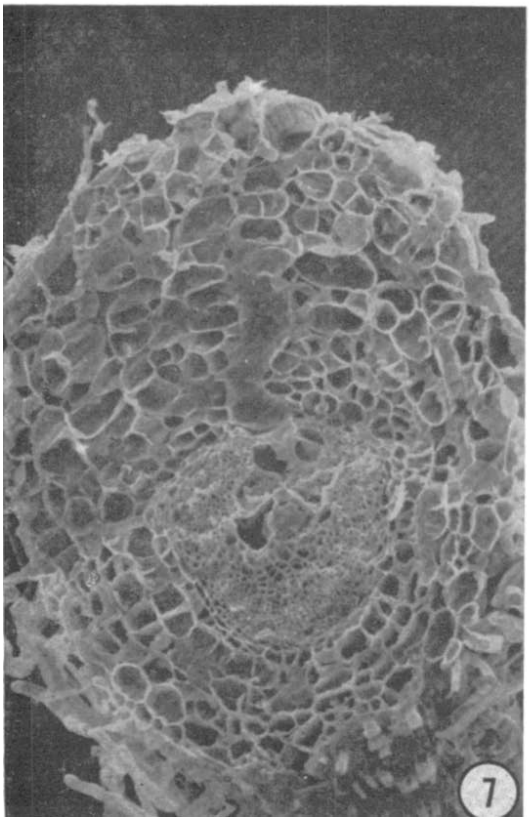
7

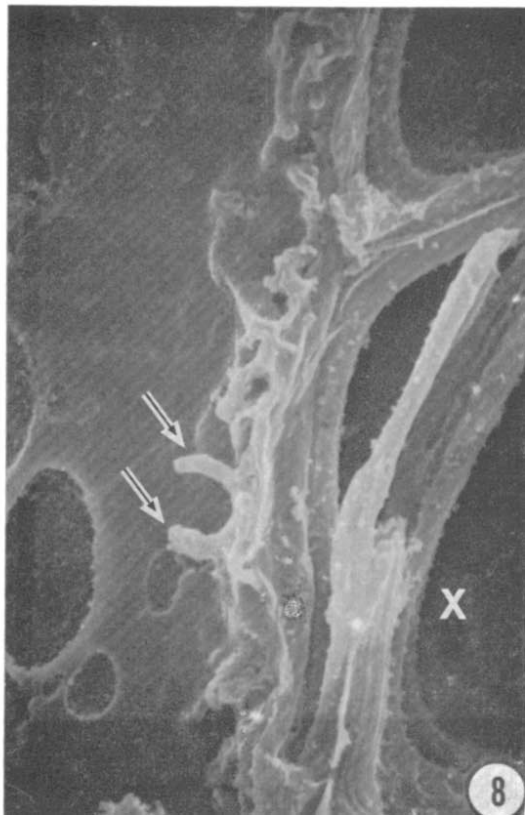
X
8

ever, the outer cell walls of the syncytia do become closely opposed by the proliferating xylem tissue (Fig. 6).

Two weeks: At 2 wk, no further development in the sizes and numbers of giant cells has occurred (Fig. 7); however, along the peripheral walls of the outer cells of the syncytia, finger-like structures can be observed that extend from the inner cell wall into the cytoplasm (Fig. 8). These wall projections, which may be irregularly shaped, are generally about 1–2 μm long and 0.5 μm in diameter. The outer walls of the syncytium become surrounded by tightly opposed xylem tissue. This tissue is characterized by reticulated (Fig. 9) and scalariform secondary wall thickenings (Fig. 10). No evidence of pits between the primary wall of the xylem and the opposing contiguous wall of the giant cells has been observed.

Three weeks: By 3 wk the nematodes have reached the fourth stage. This development is accompanied by asymmetric enlargement of the cortical region of the root that surrounds the nematode (Fig. 11). During enlargement the cells of the root are tightly appressed to the enlarging larvae. As a result, the contours of the annulae from the cuticle of the nematode are impressed on the opposing cell wall surface (Fig. 12) while the individual cell walls leave their outlines on the cuticle of the nematode (Fig. 13).

Four weeks: Asymmetrical enlargement of the cortical region of the root, which begins at 3 wk, is associated with the appearance of loosely arranged parenchyma cells on the surface of the root around the posterior end of the nematode (Fig. 14). At this time, a smooth homogeneous material accumulates between and over the surface of these root cells (Fig. 15). Fractured tissues illustrate that this material is associated with the posterior region of the nematode (Fig. 16). Consequently, it represents the gelatinous matrix that is secreted before egg laying. As this gelatinous material accumulates and egg laying begins, the loosely arranged parenchyma cells of the cortex are further displaced until the egg mass appears external to the root tissue (Fig. 17). At this time a fractured egg mass may exhibit portions of more than two dozen eggs at different stages of development (Fig. 18). When portions of the matrix are removed, intact eggs 30 × 90 μm that are characteristic of the root-knot nematode, *Meloidogyne incognita,* can be observed near the posterior end of the adult female among the parenchyma cells of the root (Fig. 19).

DISCUSSION

Structural investigations in nematology can benefit from the use of the SEM, which has a considerable depth of focus, practical resolution of at least 10 nm, and a useful magnification range extending from 20 to 20,000×. Unlike the TEM, where intracellular information results from transmitting electrons through an extremely thin (100 nm) section containing only several cells, the SEM excites electrons from the surface of much larger bulk specimens (up to 1 cm^3) to reveal topographic structural details. However, these details need not be restricted to the external surfaces of intact specimens. By utilizing a simple cryofracture technique, which does not require specialized equipment or training, the surfaces of internal tissues from fractured specimens can also be examined.

In this study, these techniques were used to re-examine the penetration of the root, differentiation of the giant cells, and development of the second-stage larvae into adult egg-laying females. The results support the generally held concept that penetration through the epidermis and cortex is largely intercellular. Within 48 h the roots exhibit the lateral swelling that was described by Christie (3) nearly 50 yr ago. This enlarge-

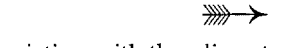

Figs. 9–10. Peripheral portions of the syncytia which exhibit close physical associations with the adjacent xylem tissue. Secondary wall thickenings of the xylem exhibit various morphological forms such as the reticulate (Fig. 9) and somewhat scalariform (Fig. 10) patterns. Although portions of the primary wall can be observed between the secondary thickenings, no obvious pits can be observed between the xylem and the syncytial cells. Fig. 9, ×900; Fig. 10, ×1250.

Fig. 11. Cryofractured root gall 3 wk after inoculation. Although the nematode is not present, its location in the distended cortical region (right) of the root is clearly evident. ×85.

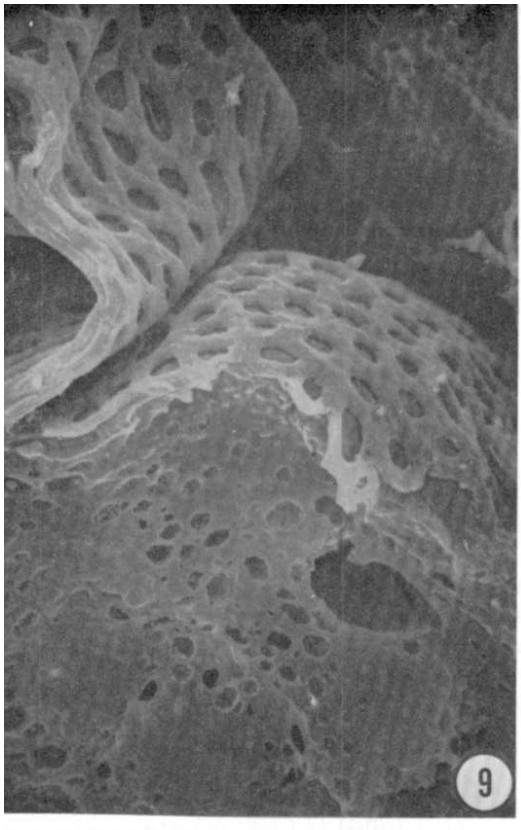
9

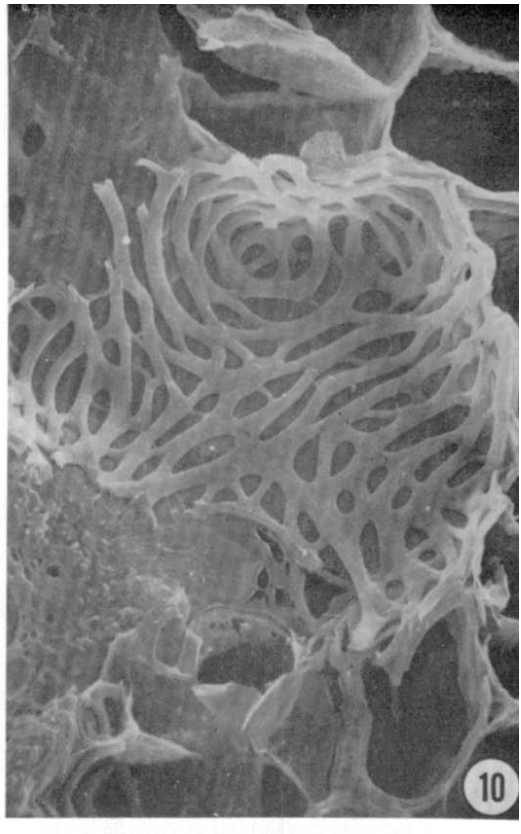
10

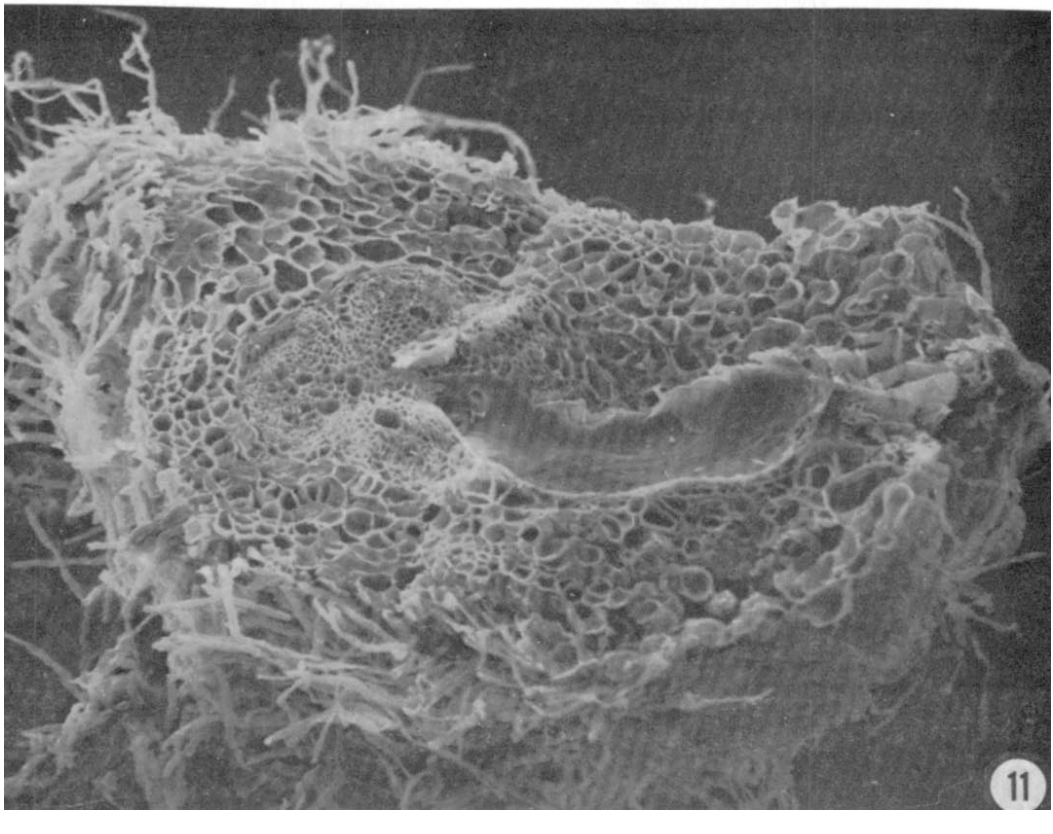
11

ment, which is easily observed in intact and fractured roots, is largely due to formation and hypertrophy of the feeding site within the vascular cylinder. In addition to the swelling, the enlarged portions of the infected roots exhibit a proliferation of root hairs. This morphological phenomenon, which undoubtedly is a secondary effect brought about by the presence and/or feeding of the nematode, may result from hormonal changes that occur in the developing gall.

Penetration of the root and development of the syncytium, as caused by the root-knot nematode, have been previously examined with the TEM (4,8,10,12). The greater resolution of this instrument has enabled investigators to document the intercellular cytoplasmic changes that occur during the early stages of infection. Although these studies have increased our understanding of the structure-function relationships that occur in the root cells, this instrument limits its observations to only a few cells. A SEM investigation of *M. incognita* (7) has concentrated on the presence and development of secondary wall ingrowths of the giant cells. Because these structures are morphologically similar to ingrowths associated with transfer cells surrounding the xylem in many normal healthy plants, the authors have suggested that the cells of the syncytium represent a specialized type of transfer cell which acts as a metabolic "sink" for the efficient accumulation of nutrients.

The current study of intact and fractured infected roots is intended to illustrate a broader view of syncytial formation and nematode development. Fractured specimens, which reveal the secondary wall ingrowths described by Jones and Dropkin (7), also illustrate the specialized xylem tissue that forms around and completely encapsulates the syncytium. This result provides further support for the concept that the syncytium functions as a metabolic "sink." Another feature well illustrated with the SEM is the morphological changes that occur in the cortex of the root as the female matures and begins to lay eggs. The parenchyma cells in the cortex appear to enlarge, loosely dissociate from one another, and finally become displaced around the outer surface of the root. These alterations, which occur prior to and during secretion of the gelatinous matrix by the nematode, may be associated with enzymatic or hormonal changes initiated by the nematode before egg laying and deserve further study.

Although the SEM has been used by nematode taxonomists for nearly 15 yr, it remains a relatively new and undeveloped technique for other disciplines in nematology. Recent development of the x-ray detector, an accessory that can be added to many standard SEMs, allows an investigator to gain qualitative and semi-quantitative data about the chemical composition of a specimen. Recently, Bird (2) has used this technique to examine ion concentrations in the nematode-induced syncytia. Atkinson et al. (1) also used the x-ray detector to show that nematode eggs exposed to a hatching stimulus contained an increased amount of calcium. As improvements are made to precipitate and immobilize salts, ions, enzymes, etc., this technique will complement structural SEM studies so that physiological and biochemical changes associated with the host-parasite interaction can also be ascertained with the SEM.

LITERATURE CITED

1. Atkinson, H. J., J. D. Taylor, and A. J. Ballantyne. 1980. The uptake of calcium prior to the hatching of the second-stage juvenile of

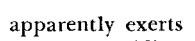

Figs. 12–13. As the nematode feeds and enlarges, the body of the developing larva apparently exerts pressure on the adjacent root cells. Evidence for this phenomenon are the annular-like patterns, resembling those on the cuticle, that can be observed on the wall of the cortical cells (Fig. 12) and the cellular outlines on the plant, which are present on the cuticle of the nematode (arrows, Fig. 13). The space (S), which can be observed between the cuticle of the nematode and the adjacent root tissue (Fig. 13), is probably an artifact that results from shrinkage during the dehydration or critical point drying procedures. Fig. 12, ×3500; Fig. 13, ×300.

Figs. 14–15. Intact portions of root galls 4 wk after inoculation. As the cortex becomes distended by the enlarging nematode, loosely associated parenchyma cells can be observed on the surface of the root (Fig 14). Following this appearance, a smooth amorphous material emerges and covers the surface of the distended cortical region (Fig. 15). Fig. 14, ×50; Fig. 15, ×100.

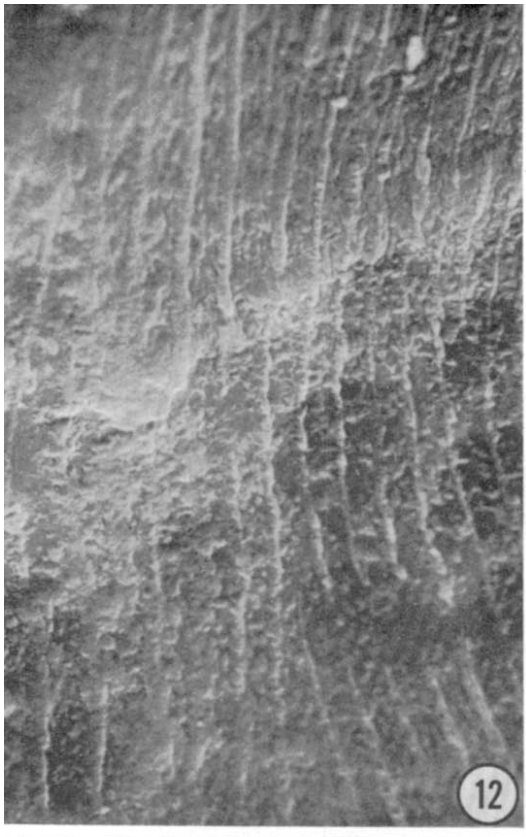
12

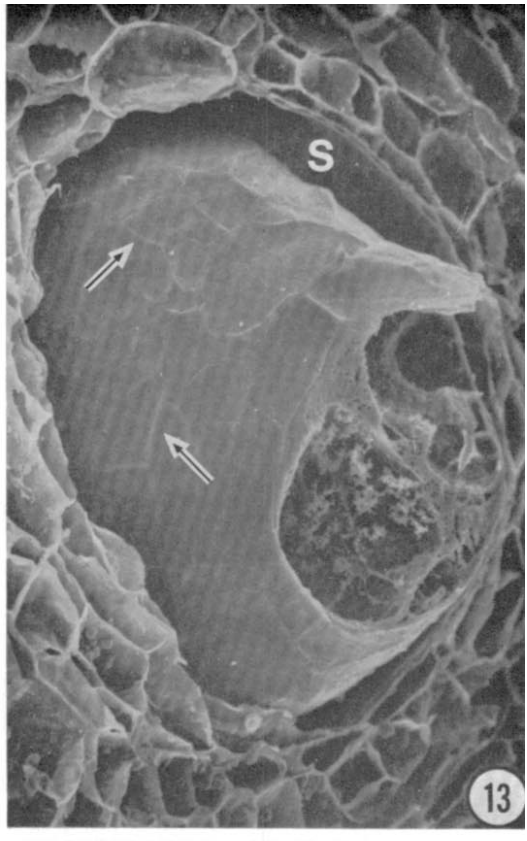
S
13

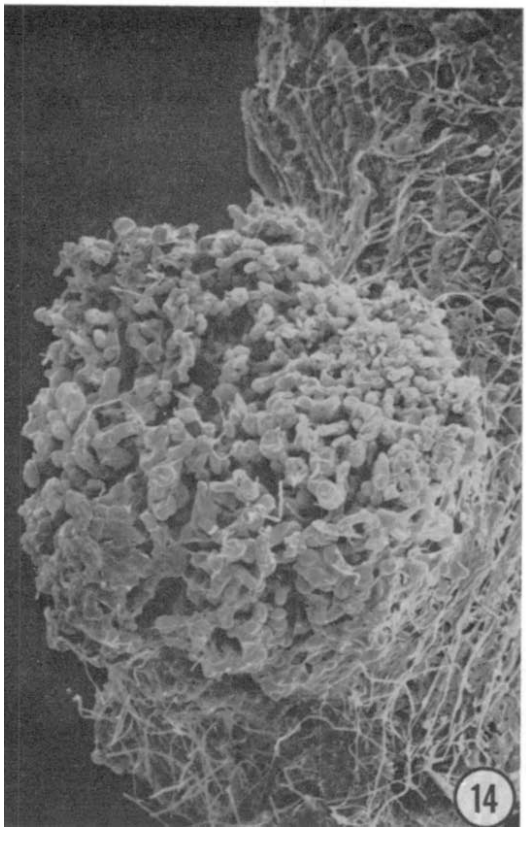
14

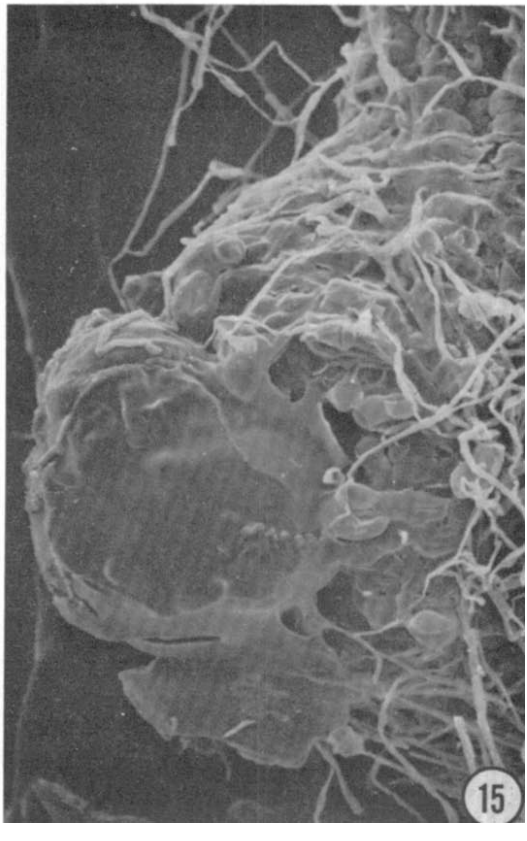
15

Globodera rostochiensis. Ann. Appl. Biol. 94:103-109.

2. Bird, A. F. 1977. The effect of various concentrations of sodium chloride on the host-parasite relationship of the root-knot nematode (Meloidogyne javanica) and soybean (Glycine max var. Lee). Marcellia 40:167-175.

3. Christie, J. R. 1936. The development of root-knot nematode galls. Phytopathology 26:1-22.

4. Endo, B. Y., and W. P. Wergin. 1973. Ultrastructural investigation of clover roots during early stages of infection by the root-knot nematode, Meloidogyne incognita. Protoplasma 78:365-379.

5. Hogger, C. H., and R. H. Estey. 1977. Cryofracturing for scanning electron microscope observations of internal structures of nematodes. J. Nematol. 9:334-337.

6. Jones, M. G. K., and V. H. Dropkin. 1975. Scanning electron microscopy of syncytial transfer cells induced in roots by cyst-nematodes. Physiol. Plant Pathol. 7:259-263.

7. Jones, M. G. K., and V. H. Dropkin. 1976. Scanning electron microscopy of nematode-induced giant transfer cells. Cytobios 15:149-161.

8. Jones, M. G. K., and D. H. Northcote. 1972. Multinucleate transfer cells induced in coleus roots by the root-knot nematode, Meloidogyne arenaria. Protoplasma 75:381-395.

9. Jones, M. G. K., and H. L. Payne. 1977. Scanning electron microscopy of syncytia induced by Nacobbus aberrans in tomato roots. Nematologica 23:172-176.

10. Jones, M. G. K., and H. L. Payne. 1978. Early stages of nematode-induced giant-cell formation in roots of Impatiens balsamina. J. Nematol. 10:70-84.

11. Orion, D., W. P. Wergin, and B. Y. Endo. 1980. Inhibition of syncytia formation and root-knot nematode development on cultures of excised tomato roots. J. Nematol. 12:196-203.

12. Paulson, R. E., and J. M. Webster. 1970. Giant cell formation in tomato roots caused by Meloidogyne incognita and Meloidogyne hapla (Nematoda) infection. A light and electron microscope study. Can. J. Bot. 48:271-276.

13. s'Jacob, J. J., and J. van Bezooijen. 1977. A manual for practical work in nematology (revised edition). Intern. Postgraduate Nematology Course, Intern. Agric. Center, Wageningen, The Netherlands.

14. Wergin, W. P., B. Y. Endo, and R. M. Sayre. 1977. Three-dimensional SEM and freeze fracture for examination of the anatomy and morphology of nematode larvae and infection sites. J. Nematol. 9: 288.

Fig. 16. Cryofractured portion of an infected root 4 wk after inoculation. The smooth homogeneous material, illustrated in Fig. 15, is present near the posterior region of the nematode. This material, which apparently corresponds to the gelatinous matrix normally secreted by the female nematode, contains portions of several eggs (arrows) which were also fractured. V = vulva. ×250.

Figs. 17–18. Cross section through an infected cryofractured root illustrating the distended cortical region of the root, the relative position of the nematode (arrow), which was partially lost during the fracture procedure, and a mature egg mass externally located on the root (Fig. 17). The egg mass contains fractured portions of eggs at different stages of development (Fig. 18). Fig. 17, ×80; Fig. 18, ×225.

Fig. 19. Portion of a root near an egg mass illustrating an intact egg characteristic of *Meloidogyne incognita*. ×450.

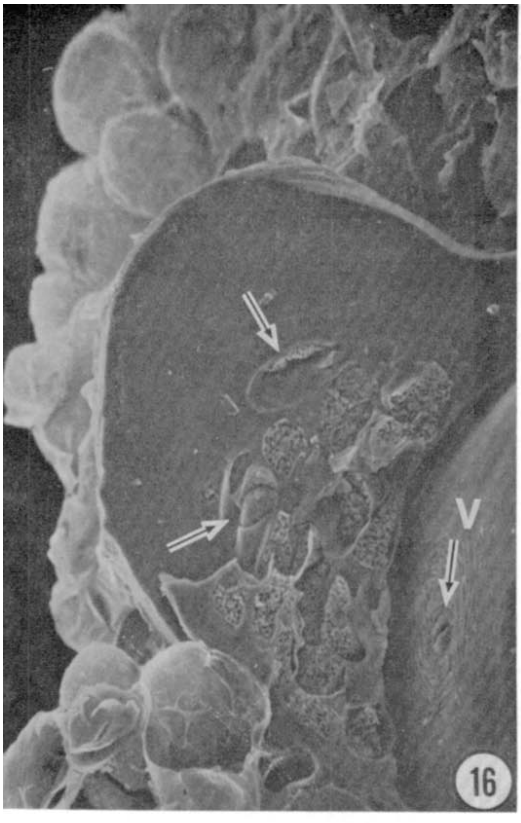
V
16

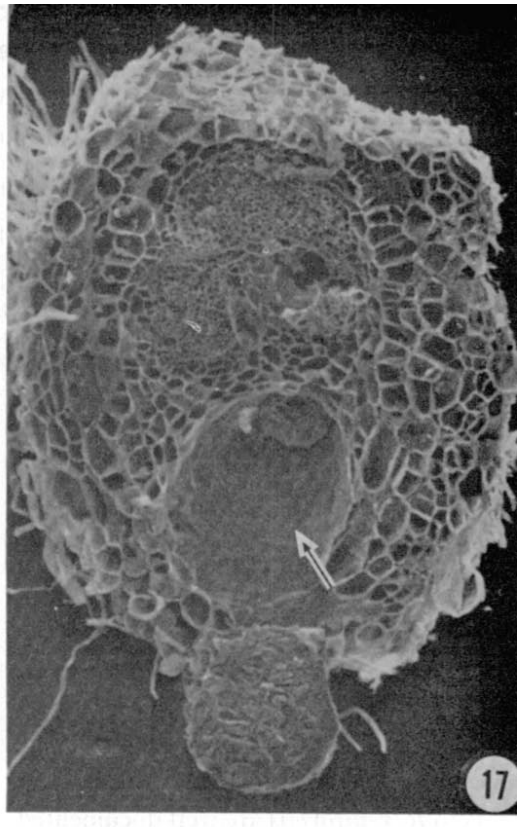
17

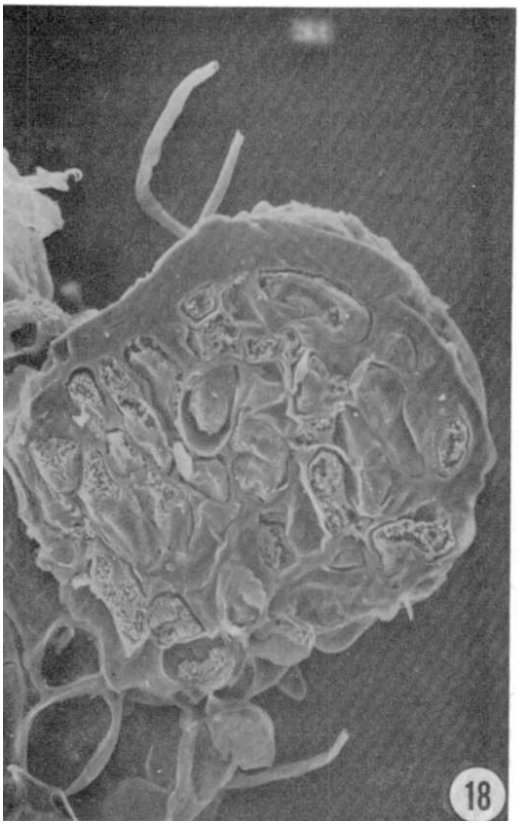
18

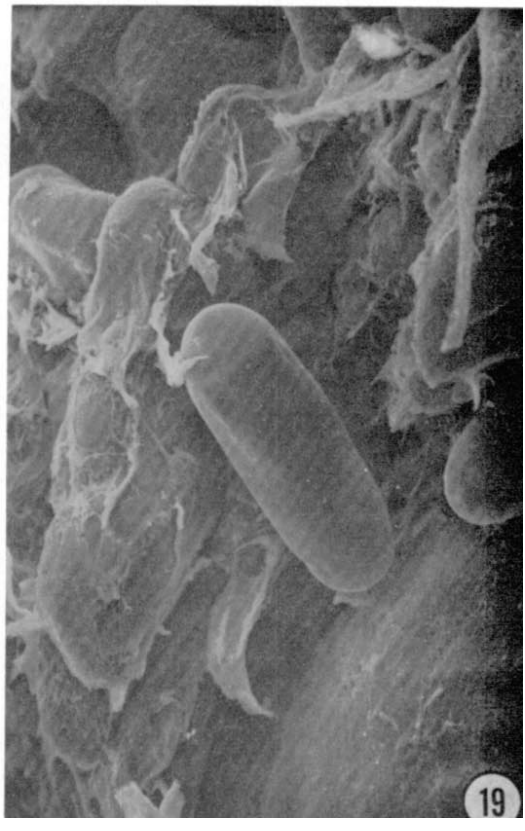
19